JOURNAL of
MATERIALS and MECHATRONICS:A

e-ISSN 2717-8811
JournalMM, 2025, 6(1), 49-67
https://doi.org/10.55546/jmm.1619158

**Araştırma Makalesi / Research Article**

# Numerical Investigation of the Flow Characteristics of Slurry Manure in a Digestion Tank

Emre Aşkın ELİBOL*

* Giresun University, Faculty of Engineering, Department of Mechanical Engineering, Giresun, Türkiye,
ORCID ID: https://orcid.org/0000-0001-8573-6065, emre.elibol@giresun.edu.tr

**Geliş/ Received:** 13.01.2025**;** **Revize/Revised:** 10.02.2025 **Kabul / Accepted:** 20.02.2025

**ABSTRACT:** Animal manure, agricultural wastes and sewage sludge are the most widely used organic wastes in biogas production. In our country, manure from animals such as cattle, sheep and chickens is an important source for biogas production. The mixing process in the digestion tank of the reactors used for biogas production significantly affects the biogas production efficiency. In recent years, it is known that the geometric structure of the digestion tank where the mixing process is carried out also affects this efficiency. In the mixing process, the most commonly used mixing type is mechanical mixing with the help of an propeller/impeller. Due to the high cost and time-consuming aspect of experimental studies, in recent years, the flow characteristics inside the digestion tank have been studied with the help of computational fluid dynamics software. In this context, velocity, turbulent eddy dissipation rate and turbulent kinetic energy distributions in the velocity range 50-175 rpm were investigated in a 60° slope digestion tank with a 6-flat-bladed impeller and the potential effects on biogas production were interpreted. The working fluid in the tank is considered by modeling dairy cattle manure as a non-Newtonian fluid. The results show that the velocity, turbulent kinetic energy and turbulent eddy dissipation rate distributions are generally more effective in the impeller region and at the impeller blade tips. In addition, as the impeller angular velocity increased from 50 rpm to 175 rpm, the amount of volume in the tank with velocity values higher than 0.1 m/s increased from 0.000323 $m^3$ to 0.00262 $m^3$.

**Keywords:** Biogas, Digester tank, Mechanical mixing, Renewable energy, CFD

*Sorumlu yazar / Corresponding author: emre.elibol@giresun.edu.tr
Bu makaleye atıf yapmak için /To cite this article

Elibol, E. A. (2025). Numerical Investigation of the Flow Characteristics of Slurry Manure in a Digestion Tank. Journal of Materials and Mechatronics: A (JournalMM), 6(1), 49-67.

## 1. INTRODUCTION

Anaerobically digesting organic waste is an economical solution for the sustainable use of energy. The mixing process is an important operation that homogenizes the anaerobic bacteria, nutrients, and temperature inside the reactor digestion tank in order to improve biogas production. Among the most common mixing methods are gas mixing, mechanical mixing, and mechanical pumping; among these, it is known that mechanical mixing is the most efficient method (Wu, 2009). The mechanical mixing process is generally carried out in a closed cylindrical tank, commonly referred to as a digester, which has a large diameter-to-height ratio. To obtain a highly efficient mixing process on an industrial scale, testing different mixing regimes in the digester to understand the physical properties of the mixing is quite costly economically. Therefore, in the study of the mixing performance of full-scale anaerobic digestion tanks, utilizing computational fluid dynamics (CFD) software is considered a highly suitable approach in terms of both cost-effectiveness and time savings (Sadino-Riquelme et al., 2018). Moreover, visualizing the flow model of the mixing process carried out in a biogas reactor using CFD software can provide researchers with information about flow behavior (Wang et al., 2018). In the future, considering the increasing energy demand and consequently the demand for biogas as a renewable energy source, it is expected that interest in the mixing process technology occurring within the reactor digestion tank will also increase. Moreover, CFD has the capability to assist in the design of the reactor digestion tank and optimal impeller/mixer designs before the actual reactor manufacturing. In this sense, it is obvious that CFD softwares will continue to be a useful tool in the development of mixing technologies. To date, studies numerically examining the effects of a broad variety of impeller types, both with and without buffles, on mechanical mixing in the reactor digestion tank have been summarized in Table 1.

**Table 1.** Literature studies investigating flow characteristics in a reactor digestion tank

| Study | Impeller type | Working fluid | Tank geometry | Buffle | Angular velocity | The parameter being examined | Main findings |
|---|---|---|---|---|---|---|---|
| (Wu, 2012) | Lightning A310 (3-pitched-bladed) | Non-Newtonian (cattle manure slurry) | Cylindrical | None | 500 rpm | Effects of different sliding mesh methods on velocity distribution in Large Eddy Simulation. | Smagorinsky–Lilly, wall-adapting local eddy viscosity and kinetic energy transfer models have shown similar flow field results. |
| (Wu, 2011) | Lightning A310 (3-pitched-bladed)<br>PMSL 3LS39 (3-pitched-bladed) | Non-Newtonian (cattle manure slurry) | Cylindrical | Exists | 250-500 rpm | The effect of 6 different turbulence models on the flow coefficient. | In the cases where the total solid content (TS) = 7.5% and TS = 12%, the standard k-ε, RNG k-ε, and realizable k-ε models yielded higher mixing flow coefficients compared to the other models. |
| (Wu, 2010) | 2-spiral-bladed | Non-Newtonian (cattle manure slurry) | Bulb-shaped<br>Cylindrical | None | 400-750 rpm | The difference has compared various turbulence models in different TSs in terms of mixing intensity levels. | It has been stated that the mixing density level ($W/m^3$) of the bulb-shaped tank geometry is more efficient compared to the cylindrical one. |
| (Wu, 2009) | 2-spiral-bladed | Newtonian (water)<br>Non-Newtonian (cattle manure slurry) | Cylindrical | None | 216-410 rpm | The effect of the impeller's position inside the tank on the velocity distribution. | In the case of TS ≤ 5.4%, a homogeneous velocity distribution was observed for all examined cases. |

**Tablo 1.** Literature studies investigating flow characteristics in a reactor digestion tank (continued)

| Study | Impeller type | Working fluid | Tank geometry | Buffle | Angular velocity | The parameter being examined | Main findings |
|---|---|---|---|---|---|---|---|
| (Abu-Farah et al., 2010) | Rushton (6-flat-bladed) | Newtonian (Cyclohexane/water mixture) | Cylindrical | None | 350-750 rpm | The effect of different impeller angular velocities on velocity distribution. | -It has been observed that the standard k-ε turbulence model is quite close to the experimental dispersion behavior.<br>-It has been determined that the minimum impeller velocity for complete dispersion is approximately 550 rpm. |
| (Bridgeman, 2012) | 2 pieces of 2-flat-bladed | Non-Newtonian (sewage slurry) | Cylindrical | None | 20-200 rpm | -The effect of TS content on dead zone volume.<br>-The effect of different impeller angular velocities on the velocity gradient. | -They have observed that as TS increases, the volume of the dead zone inside the tank also increases.<br>-Even with the increase in impeller velocity from 100 rpm to 200 rpm, very little change has been observed in the turbulence characteristics of the flow field (1/s). |
| (Shen et al., 2013) | 1 pieces of 2-pitched-bladed<br>2 pieces of 2-pitched-bladed<br>3 pieces of 2-pitched-bladed | Non-Newtonian (rice straw slurry) | Cylindrical | None | 20-160 rpm | The effects of different impeller designs and numbers on the velocity and turbulence kinetic energy (TKE) distribution within the tank have been examined at different angular velocities. | -They stated that 3 pieces of 2-pitched-bladed impeller at 80 rpm provided better results in terms of the affected volume ratio in the tank.<br>-They observed that the TKE increased from 0.014 $m^2/s^2$ to 0.02 $m^2/s^2$ as the angular velocity increased from 120 rpm to 160 rpm. |
| (Sindall et al., 2013) | 4-flat-bladed | Non-Newtonian (sewage slurry) | Cylindrical | Exists (4 pieces) | 50-200 rpm | Effects of angular velocity on the velocity gradient. | It has been stated that within the examined angular velocity range, the velocity gradient is less than 10 $s^{-1}$ in 20%-85% of the tank. |

**Tablo 1.** Literature studies investigating flow characteristics in a reactor digestion tank (continued)

| Study | Impeller type | Working fluid | Tank geometry | Buffle | Angular velocity | The parameter being examined | Main findings |
|---|---|---|---|---|---|---|---|
| (Rasool et al., 2017) | Chemineer S-4 (4-bladed)<br>4-pitched-bladed<br>Spiral-bladed | Newtonian (water) | Cylindrical | Exists (4 pieces) | 60-135 rpm | The effect of the impeller type and angular velocity on the velocity distribution. | The pitched-bladed impeller has created a smaller weak mixing zone compared to the Chemineer impeller. |
| (Cao et al., 2018) | 2 pieces of 3-pitched-bladed | Non-Newtonian (mud slurry) | Cylindrical<br>Oval | None | 10-40 rpm | The effect of tank geometry and angular velocity on velocity distribution and dead zone volume. | -In TS = 4% and 40 rpm conditions, they observed that the dead zone volume was smaller.<br>-The results of both tank geometries are similar in terms of velocity distribution. |
| (Oates et al., 2020) | 2 pieces of 3-pitched-bladed in addition to 1 pieces of 2-pitched-bladed<br>Spiral-bladed | Non-Newtonian (water-glycerin mixture) | Cylindrical | None | 2.5-12 rpm | The effects of different impeller designs and TSs on the velocity distribution and the affected volume ratio of the tank have been examined. | -The affected volume ratio of the tank is highest at 60%-98% (TS = 2.5%) when using a spiral-bladed impeller; it is highest at 12%-67% (TK = 5.4%) when using the other configuration. |
| (Servati and Hajinezhad, 2020) | 4-flat-bladed | Non-Newtonian (mud slurry) | Cylindrical | Exists (4 pieces) | 50-200 rpm | The effect of angular velocity on velocity, TKE, turbulence intensity, and velocity gradient distribution. | -The dead zone volume has been determined to be 10% within the examined angular velocity range.<br>-The turbulence intensity distribution is similar at all angular velocities.<br>- The turbulence intensity is less than 10%-20% in areas close to the tank walls; 20%-30% in the rotating part, and 10% in the other part. |

**Tablo 1.** Literature studies investigating flow characteristics in a reactor digestion tank (continued)

| Study | Impeller type | Working fluid | Tank geometry | Buffle | Angular velocity | The parameter being examined | Main findings |
|---|---|---|---|---|---|---|---|
| (Hoseini et al., 2021) | Rushton (6-flat-bladed)<br>6-V shape-bladed<br>6-U shape-bladed | Newtonian (water) | Cylindrical | Exists (4 pieces) | 201-401 rpm | The effect of different impeller designs and angular velocities on the distribution of velocity, TKE, and turbulence eddy dissipation rate (TED). | -The highest TKE value was obtained in the Rushton impeller.<br>- The highest TED ratio value was obtained for the 6-U shape-bladed impeller.<br>-The highest radial velocity value was obtained in the Rushton impeller. |
| (Thakur et al., 2023) | 1 pieces of 2-flat-bladed<br>2 pieces of 4-flat-bladed | Non-Newtonian (sewage slurry) | Cylindrical | None | 50-600 rpm | The effect of different designs, different TSs, and different angular velocities on the dead zone volume and velocity distribution. | -They have observed that the volume of the dead zone decreases with the increase in angular velocity.<br>-When using 2 pieces of 4-flat-bladed impeller, the maximum velocity value increases. |
| (Celik et al., 2024) | Rushton (6-flat-bladed) | Newtonian (water) | Cylindrical | None | 25-100 rpm | The effect of tank geometry and impeller angular velocity on the distribution of velocity, TKE, TED ratio, and dead zone volume. | -In the case of using a 60° slope tank, they observed that the dead zone volume decreased and the maximum velocity, TKE, and TED ratio increased. |

For biogas production, animal (cattle, sheep, poultry, slaughterhouse waste, etc.), plant, household, and industrial wastes are commonly used. These wastes are mixed with water to form a slurry and then transferred to the reactor digestion tank. Here, during the mechanical mixing process of the slurry, the slurry waste is broken down by bacteria present in an anaerobic environment, resulting in a mixture of methane, carbon dioxide, and other gases known as biogas. Since the slurry in question behaves like a non-Newtonian fluid, its thermophysical and rheological properties must be accurately defined in the computational domain generated by CFD. Otherwise, using the input parameters (impeller angular velocity, impeller geometry, tank geometry, etc.) in the simulation, the results obtained from the simulations cannot be expected in practice. However, of course, by defining a Newtonian fluid like water in the reactor digestion tank, it can be determined which type of impeller or which tank geometry is more effective with CFD. As seen in Table 1, some researchers have numerically examined the flow behavior inside the reactor slurry tank, modeling the working fluid as Newtonian, while others have modeled it as a non-Newtonian fluid. Although a very wide range of impeller angular velocities is generally adopted in the literature, simulations have mostly been conducted for the traditional 90° slope (cylindrical) tank geometry. However, in a very recent study (Celik et al., 2024), it is stated that the dead zone volume decreases when using a 60° slope tank geometry compared to using a traditional 90° slope (cylindrical) tank geometry. Additionally, no study has been found that addresses dairy cattle manure as the working fluid in terms of thermo-physical and rheological properties. The modeling of the working fluid in the reactor tank as a real manure slurry is another unique aspect of the current study, especially providing an insight for researchers working in the field of biogas.

In order to address the lack of literature on the subject, in this study, dairy cattle manure was modelled as a non-Newtonian fluid in a 60° slope and 4 buffles reactor digestion tank with a 6-flat-bladed Rushton impeller and the flow behaviour inside the tank at different impeller angular velocities was numerically investigated (with ANSYS Fluent software) in terms of velocity distribution, TKE and TED rate.

## 2. MATERIALS AND METHODS

### 2.1 Physical Model and Computational Domain

The geometric dimensions and schematic view of the reactor digestion tank and the 6-flat-bladed impeller inside it are shown in Figure 1. There are four buffles with the same geometric dimensions on the tank wall. The impeller is mounted accurately in the center of the tank. The 3D view of the computational domain consisting of the tank and impeller is shown in Figure 2. The choice to set the impeller's angular velocity at 175 rpm or below is due to the possible danger that increased velocities might harm microbiological organisms in practical terms, hence negatively affecting biogas production.

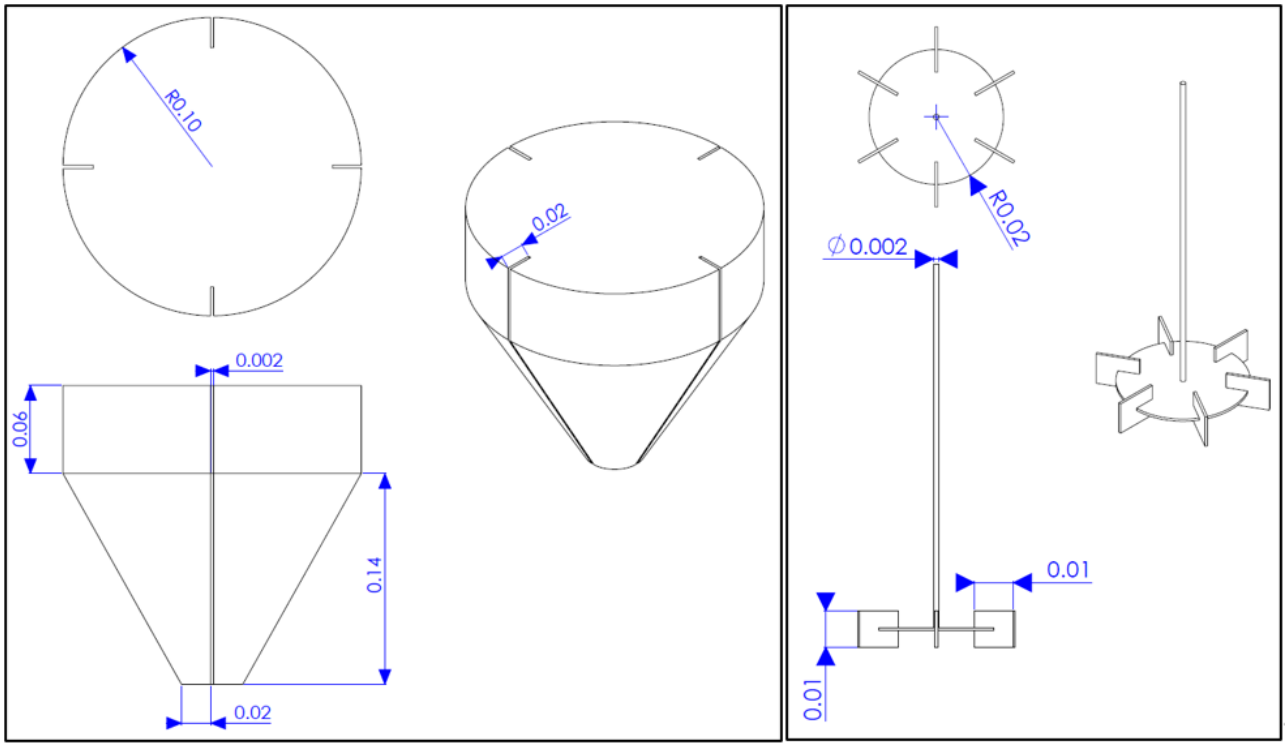


**Figure 1.** Geometric dimensions and schematic view of the tank and impeller

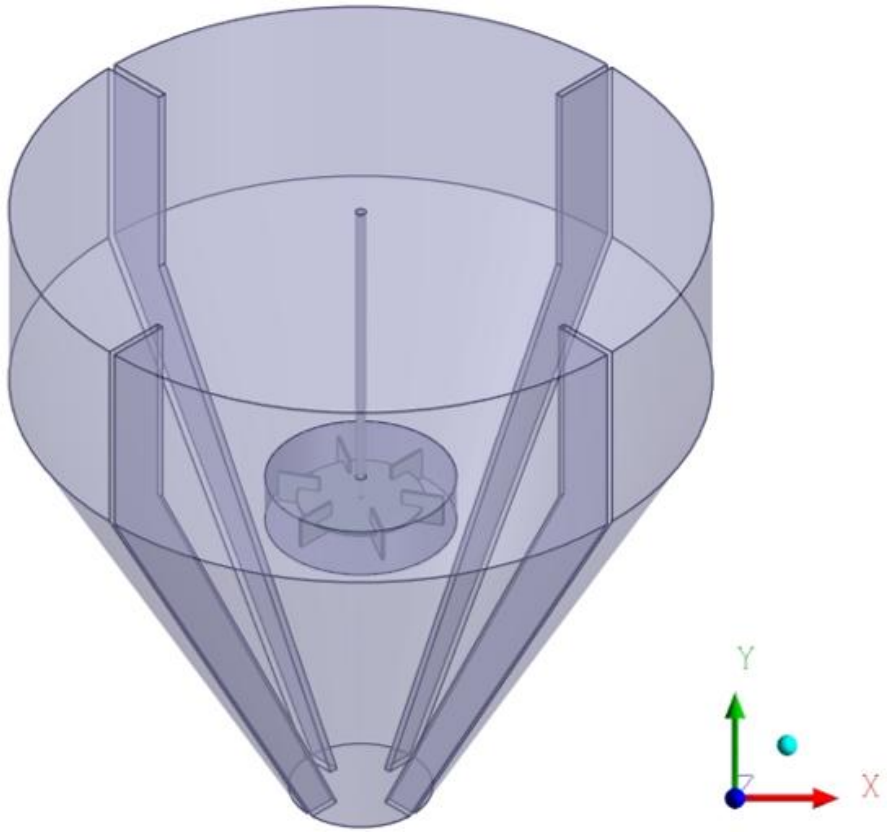


**Figure 2.** 3D view of the computational domain consisting of tank and impeller

### 2.2 Thermo-physical and Rheological Properties of Dairy Cattle Manure

The rheological and thermo-physical properties of the working fluid were calculated at T = 298 K and TS = 12%. Within the parameters of total solids ranging from 2.5% to 12% and temperatures stretching from 20°C to 60°C, dairy cattle manure exhibits characteristics of a pseudoplastic fluid. Given these parameters, it's possible to derive the consistency coefficient (K) and the behavior index through the following calculations (Achkari-Begdouri and Goodrich, 1992):

$$K = \left(8.722e^{(4830/T)+0.58319(TS)}\right) \times 10^{-10} \tag{1}$$

$$n = 0.6894 + 0.0046831(T - 273) - 0.042813(TS) \tag{2}$$

Here, the temperature, T, is in Kelvin and TS is in percent.

For the range of 10% to 50% of TS, the density of dairy cattle manure can be calculated as follows (Wang et al., 2019):

$$\rho = 0.0367(TS)^3 - 2.38(TS)^2 + 14.6(TS) + 1000 \tag{3}$$

### 2.3 Governing Equations

Since it was assumed that the temperature inside the reactor digestion tank is constant, the energy conservation equation was not taken into account. Additionally, it has been assumed that the flow inside the tank is steady. In this way, the continuity equation in the rotating reference frame of the reactor tank can be expressed as follows:

$$\nabla \cdot \vec{V} = 0 \tag{4}$$

With the same assumptions, the momentum equations (Mousavi et al., 2019) for the stationary part of the reactor tank (inertial reference frame) and the rotating part (rotating reference frame) are respectively shown in Equation 5 and Equation 6:

$$\rho\nabla\left(\vec{V}\vec{V}\right) = -\nabla p + \nabla \cdot \tau + \rho\vec{g} \tag{5}$$

$$\rho\nabla\left(\vec{V}\vec{V}\right) = -\nabla p + \nabla \cdot \tau + \rho\vec{g} + \vec{F} \tag{6}$$

The expression on the left side of Equation 5 and Equation 6 denotes the convective (local) acceleration. The initial, subsequent, and tertiary terms on the right side of both equations denote the pressure gradient, internal stress forces (viscous effects), and external body forces (attributable to gravitational influence), respectively. The fourth term of Equation 6, denoted as F, represents the force arising from the rotating reference frame (the added/body forces acting on the fluid).

The shear stress, τ, in Equation 5 and Equation 6 can be expressed as follows:

$$\tau = \mu_{eff}\left[\left(\nabla\vec{V} + \nabla\vec{V}^T\right) - \frac{2}{3}\nabla\vec{V}I\right] \tag{7}$$

### 2.4 Turbulence Model

The standard k-ε turbulence model was used to describe the turbulent flow inside the reactor tank. The turbulent kinetic energy (k) equation and turbulent eddy dissipation rate (ε) equation (Launder and Spalding, 1972; Versteeg and Malalasekera, 2007) for the standard k-ε turbulence model are as follows, respectively:

$$\rho\nabla\left(\vec{V}k\right) = \nabla\left(\frac{\mu_T}{\sigma_k}\nabla k\right) + G_k - \rho\varepsilon \tag{8}$$

$$\rho\nabla\left(\vec{V}\varepsilon\right) = \nabla\left(\frac{\mu_T}{\sigma_\varepsilon}\nabla\varepsilon\right) + \frac{\varepsilon}{k}(C_{1\varepsilon}G_k - C_{2\varepsilon}\rho\varepsilon) \tag{9}$$

Here, $G_k$ is the turbulence due to shear (which can also be caused by mean velocity gradients), $\sigma_k$ is the turbulence Prandtl number for k. $\sigma_\varepsilon$ is the turbulence Prandtl number for ε, and $C_{1\varepsilon}$ and $C_{2\varepsilon}$ are the associated constants. The values of turbulence related constants $C_{1\varepsilon}$, $C_{2\varepsilon}$, $\sigma_k$ and $\sigma_\varepsilon$ in the standard k-ε turbulent model are 1.44, 1.92, 1.0 and 1.3, respectively. Also, $\mu_T$ is the eddy viscosity and can be expressed as:

$$\mu_T = \rho C_\mu \frac{k^2}{\varepsilon} \tag{10}$$

Here, $C_\mu$ equals to 0.09.

In the computational domain, a non-slip boundary condition was applied on the outer and lower surfaces of the tank. Furthermore, the rotating and stationary parts were automatically connected to each other (interfaces) by means of a general connection boundary condition.

### 2.5 Non-Newtonian Fluid Model

Slurry fluids with TS ≥ 2.5% can be defined as non-Newtonian pseudoplastic fluids. k-ε turbulence model was originally derived for Newtonian fluids. However, it can be extended to non-Newtonian fluids with some modifications. The 'power law' model is a simplified rheological model often used to describe the non-Newtonian behaviour of fluids, especially those exhibiting shear thinning or shear thickening behaviour. There are other mathematical models for modelling non-Newtonian fluids in the literature, such as Carreau (Carreau et al., 2021). In the 'power law' model, the inherent viscosity, μ, can be determined at each point in the flow field. The model for the inherent viscosity of dairy cattle manure in slurry form, which is considered as a non-Newtonian fluid, can be expressed as follows (Wu and Chen, 2008):

$$\mu = K(\dot{\gamma})^{n-1} \tag{11}$$

Here, K is the coefficient of consistency (a measure of the average viscosity of the fluid), $\dot{\gamma}$ is the shear per unit time and n is the behaviour/power law index (a measure of the deviation of the fluid from Newtonian behaviour). In this study, n < 1, i.e. the fluid class is shear-thinning (pseudoplastics) flow.

$$\mu_{eff} = \frac{\mu}{\mu_T} \tag{12}$$

### 2.6 Numerical Procedure and Mesh Structure

The computational domain is comprised of two distinct components: the inner section, which encompasses the rotating space, and the outer section, which contains the fixed volume of the remaining stirred tank reactor. To delineate the inner section, the Sliding Mesh (SM) technique was employed, resulting in the partitioning of the computational domain into two distinct components. One component engages with the stirrer, whereas the other remains in a state of rest. The COUPLED algorithm, one of the pressure-velocity conjugate solution options, was used since faster convergence was desired. The second order Upwind method was used to discretize the conservation equations, while the first order Upwind method was used to discretize the turbulence model equations. The residue criteria of the equations were set to $10^{-5}$.

By comparing the results obtained from different mesh numbers, the optimal number of cells for the accurate solution was determined as 8165238. A sample tetrahedral mesh structure is shown in Figure 3.

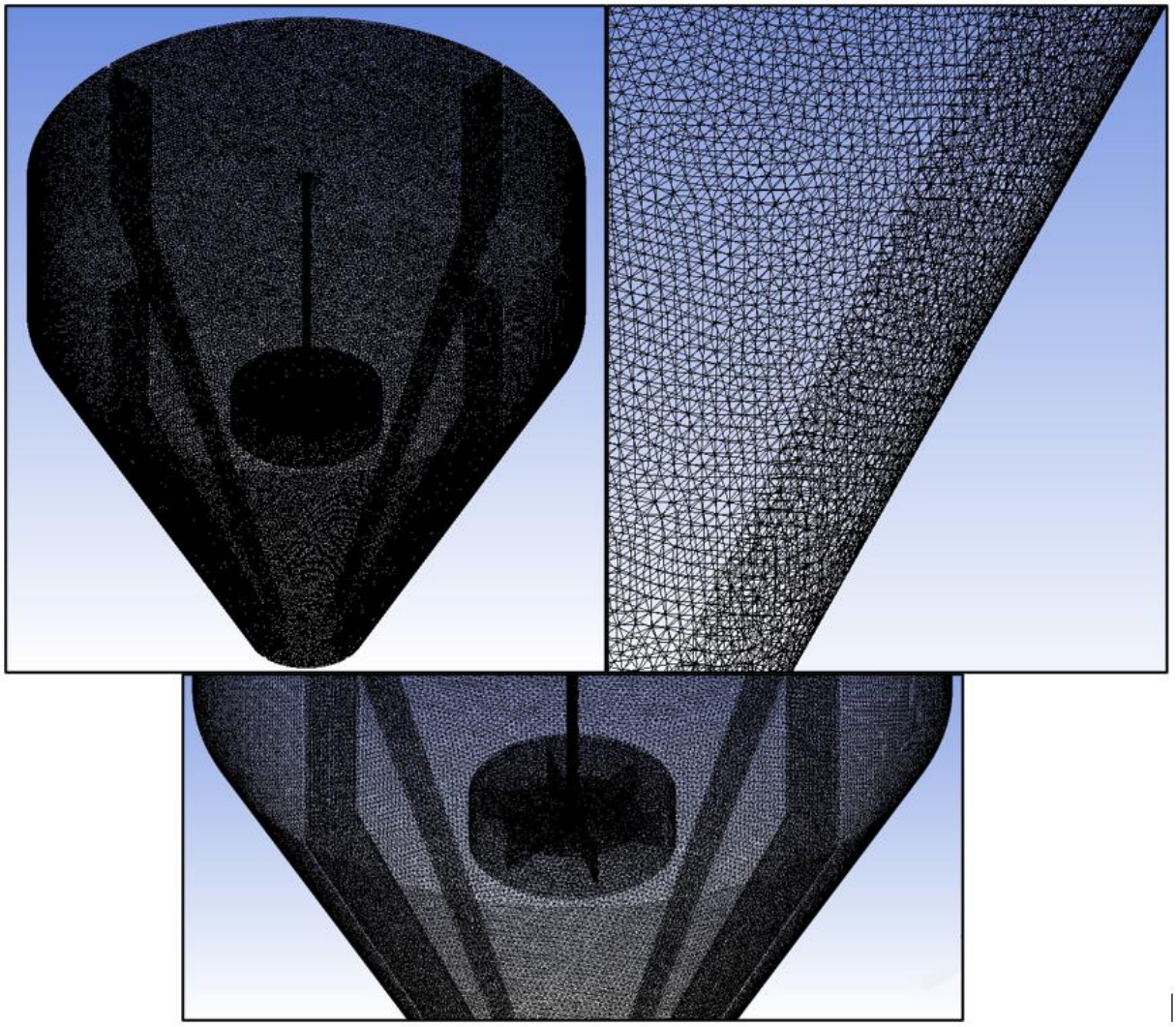

**Figure 3.** Mesh structure in an example solution

### 2.7 Model Validation

Before proceeding to the original part of the current study, the results were verified by adopting the same configurations based on the literature study (Celik et al., 2024) that was performed as a numerical. As shown in Figure 4, both studies are compared with regards to dead zone volume.

Accordingly, it is seen that the dead zone volume obtained in this study and the dead zone volume in the aforementioned literature study are very close to each other (≤ 10%).

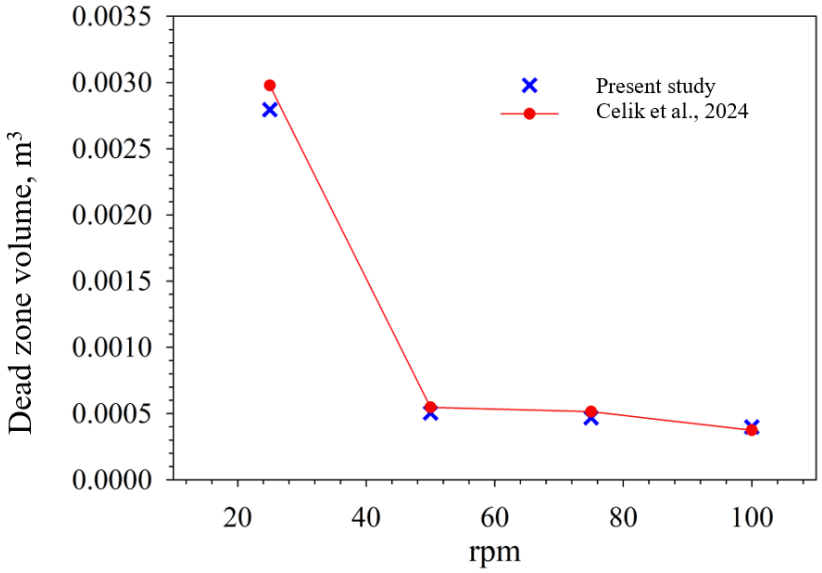


**Figure 4.** Variation of dead zone volume with respect to impeller angular velocity

## 3. RESULTS AND DISCUSSION

Figure 5 shows the velocity distribution obtained for different angular velocities of the impeller. Given that the fluid motion along the axial direction significantly influences the overall mixing within the digester tank, the axial velocity at the central vertical surface was selected to illustrate the simulation results. As expected, the maximum velocity value inside the reactor tank increases with increasing angular velocity. It can also be seen that the velocity variations in the impeller region are more effective, similar to those in the literature (Bridgeman, 2012). The maximum velocities in the selected plane are 0.608, 0.891, 1.200, 1.507, 1.818 and 2.126 m/s for 50, 75, 100, 125, 150 and 175 rpm angular velocities of the impeller, respectively. Near the bottom of the reactor digester tank, the velocity is lower, so much so that it is almost stagnant. The possible reason for this is that the non-Newtonian fluid in these areas is subjected to relatively low driving forces due to the impeller. In this case, stagnant regions are formed, resulting in a weak mixing effect in localised areas. Furthermore, the use of buffles on the tank walls has helped to reduce to some extent the low mixing zones that can occur on a tank wall without buffles (see literature studies (Hoseini et al., 2021; Celik et al., 2024)).

In order to understand whether an effective mixing is provided in the reactor tank, the velocity value of 0.1 m/s is determined as the critical velocity and the volume occupied by these regions in the reactor tank for 50 and 175 rpm values are presented in Figure 6. Accordingly, the volume with velocity values above the critical velocity for 50 rpm angular velocity is 0.000323 $m^3$ while this value is 0.00262 $m^3$ for 175 rpm angular velocity.

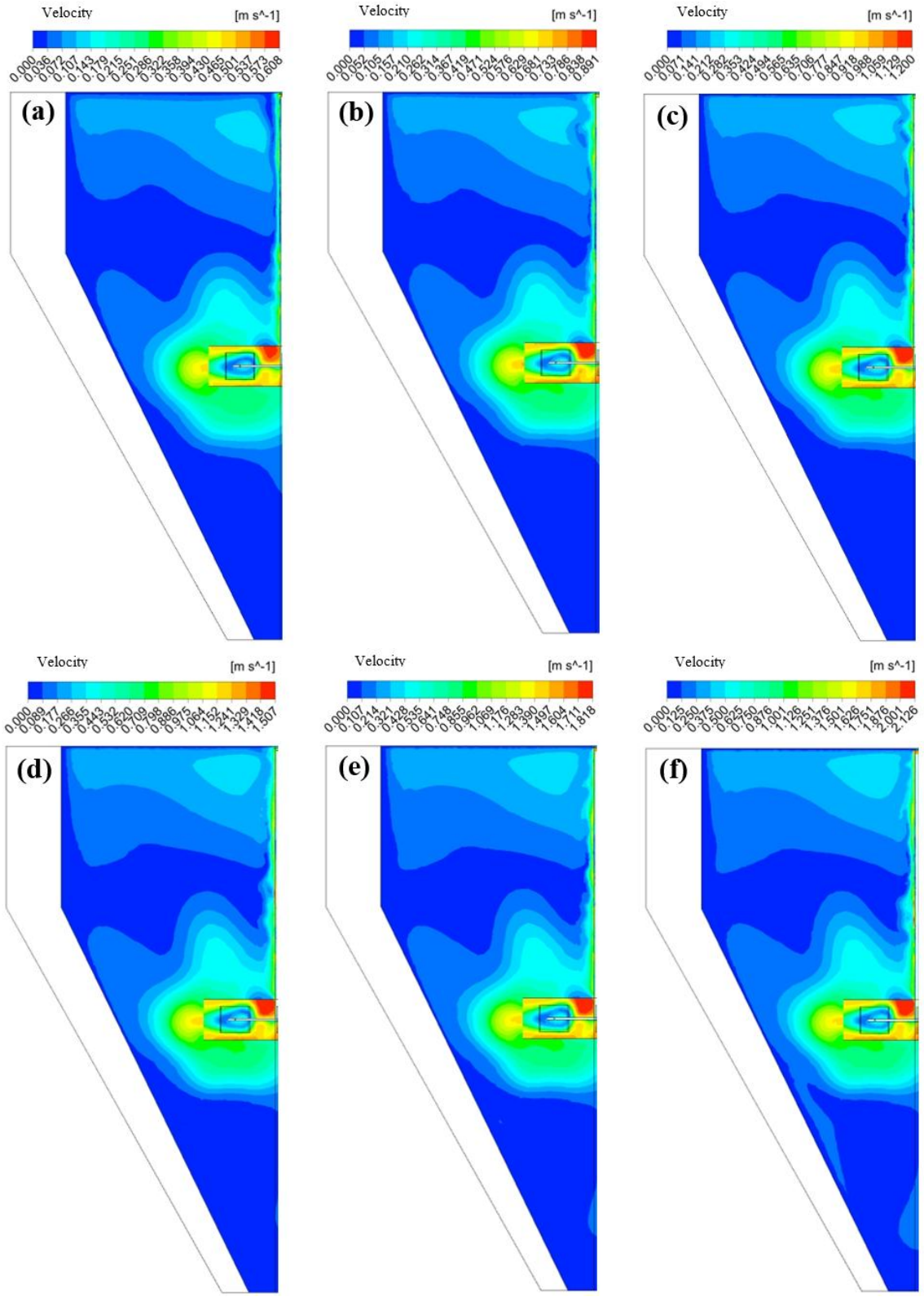


**Figure 5.** Side view of velocity distribution at different angular velocities: (a) 50 rpm, (b) 75 rpm, (c) 100 rpm, (d) 125 rpm, (e) 150 rpm and (f) 175 rpm

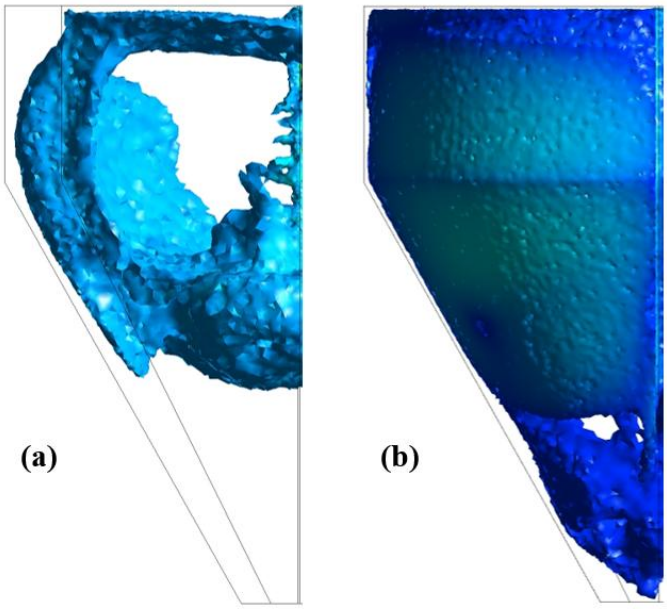


**Figure 6.** Side view of the volume inside the tank at different angular velocities where the velocity is higher than 0.1 m/s: (a) 50 rpm and (b) 175 rpm.

Figure 7 shows the turbulence kinetic energy distribution obtained for different angular velocities of the impeller. Similar to the velocity distribution, the TKE is more effective in the regions close to the impeller and the impeller shaft wall. In the other literature studies (Shen et al., 2013; Kong et al., 2014), it has also observed that the TKE distribution and magnitude are more intense and larger in the rotating part, i.e. close to the impeller, and become more sparse and smaller in the regions away from these regions. The maximum TKE in the selected plane is 0.063, 0.140, 0.140, 0.247, 0.382, 0.382, 0.535 and 0.715 $m^2/s^2$ for angular velocities of 50, 75, 100, 125, 150 and 175 rpm, respectively. The turbulence kinetic energy (TKE) equation incorporates physical terms that indicate TKE arises from the interaction of microbiological organisms within the slurry in the tank, influenced by turbulence during the mixing process. Consequently, in the analysis of flow characteristics, it is essential to consider the turbulent kinetic energy (TKE), as it directly influences the efficiency of mixing.

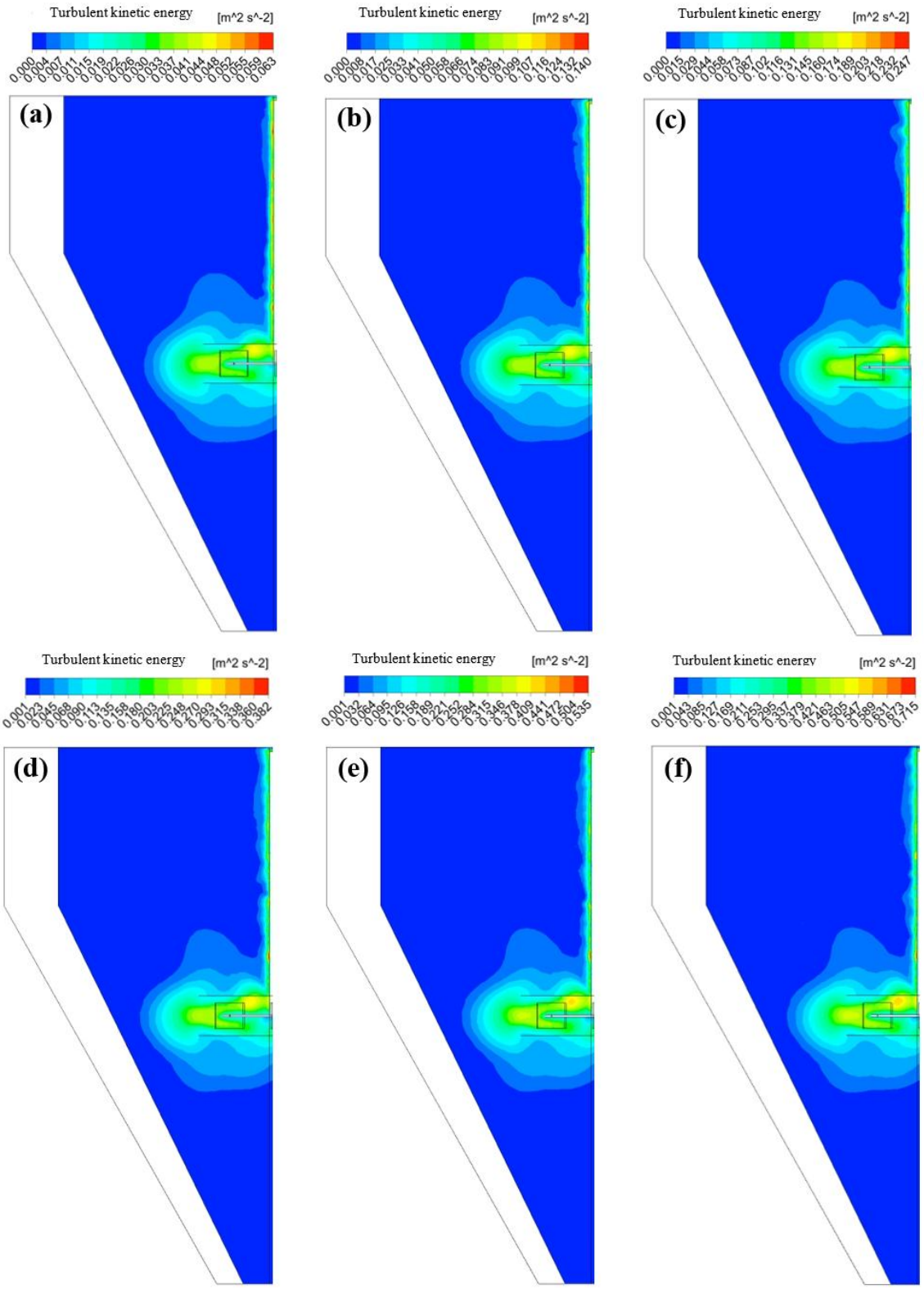


**Figure 7.** Side view of TKE distribution at different angular velocities: (a) 50 rpm, (b) 75 rpm, (c) 100 rpm, (d) 125 rpm, (e) 150 rpm and (f) 175 rpm.

Figure 8 shows the TED rate distribution obtained for the angular velocity range of 50-175 rpm. According to the figure, the maximum TED rate is 47.210, 112.634, 245.653, 456.622, 757.008 and 1169.555 $m^2/s^3$ for angular velocities of 50, 75, 100, 125, 150 and 175 rpm, respectively. The figure clearly illustrates the buffles used on the tank walls ensured that the TED rate distribution is effective in almost most regions in the considered plane. There are other studies in the literature (Fan et al.,

2015, Vilardi and Verdone, 2020) which observe that the TED rate distribution is more effective in the rotating region. Considering that a high TED rate is a measure of the rate at which TKE is converted into heat (internal energy) due to viscous losses (viscous dissipation), it can be considered that it can provide a positive effect for biogas production.

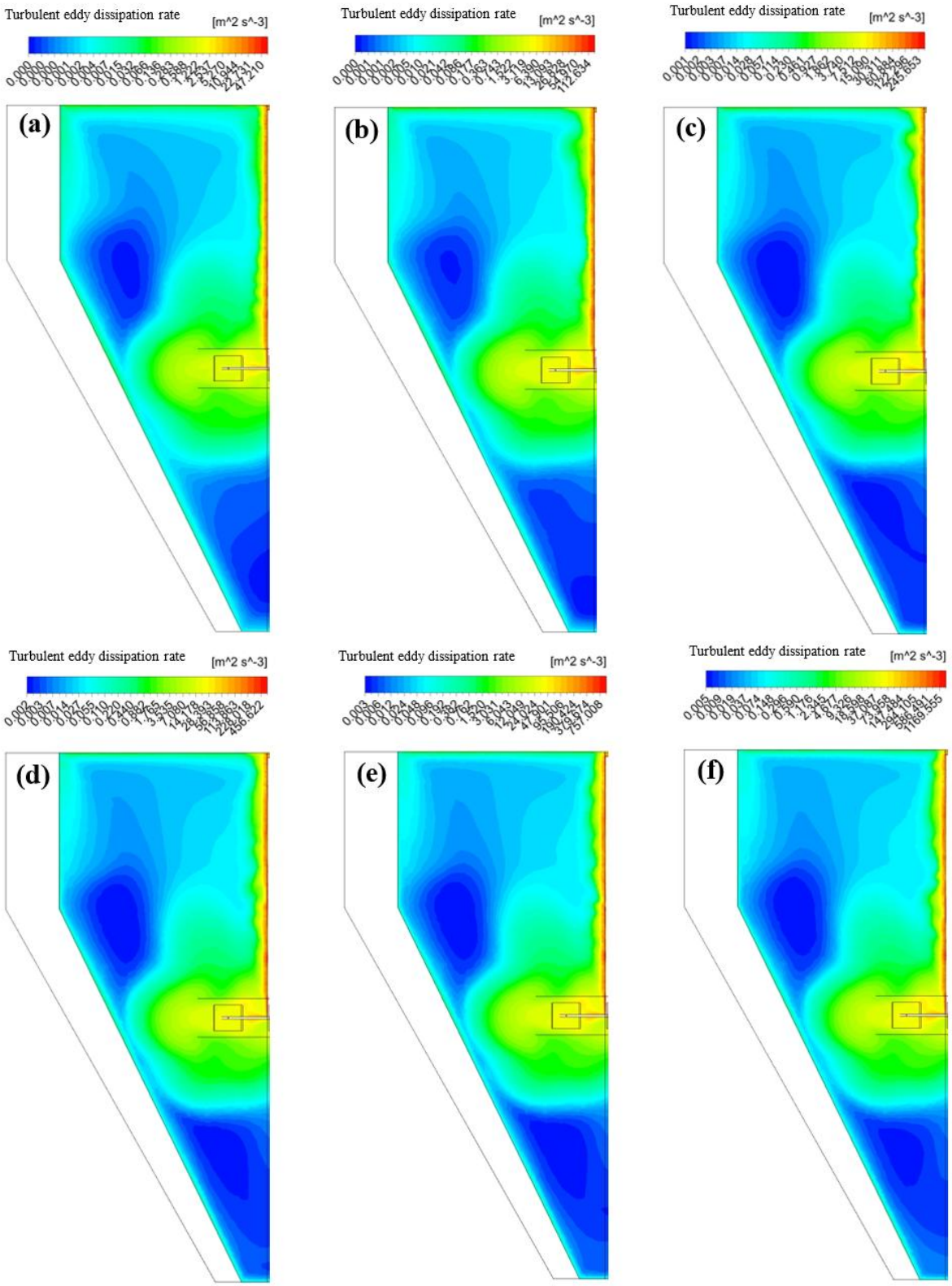


**Figure 8.** Side view of TED rate distribution at different angular velocities: (a) 50 rpm, (b) 75 rpm, (c) 100 rpm, (d) 125 rpm, (e) 150 rpm and (f) 175 rpm.

## 4. CONCLUSIONS

In this study, dairy cattle manure was modelled as a non-Newtonian fluid in a biogas reactor digester tank with a 60° slope and 4 buffles, and the flow behaviour in the tank at different angular velocities of a 6-flat-bladed Rushton impeller was numerically investigated. The thermo-physical and rheological properties of dairy manure were considered at 298 K and TS = 12%. The results were presented in terms of velocity, TKE and TED rate distributions. Some important findings obtained from the study can be listed as follows:

- It was observed that the velocity distribution was not effective in the lower parts of the impeller zone in the digester tank. For more effective mixing process in the lower parts, the impeller angular velocity should be selected higher than 175 rpm.
- By increasing the impeller angular velocity from 50 rpm to 175 rpm, the amount of volume in the tank with velocities higher than the critical velocity value of 0.1 m/s increased by approximately 710%, i.e. the dead zone volume was greatly reduced, resulting in a more effective mechanical mixing process in the tank. The volume with velocity values above the critical velocity for 50 rpm angular velocity is 0.000323 $m^3$ while this value is 0.00262 $m^3$ for 175 rpm angular velocity.
- Considering the results of the studies carried out in the literature for the reactor digester tank without an buffle, the use of buffles provided a more effective TKE and TED rate distribution near the tank walls.

Viscosity-induced losses, which significantly affect the turbulence behaviour in non-Newtonian fluids, can cause local temperature increase especially at high impeller angular velocities. Moreover, these local temperature changes may affect the thermo-physical and rheological properties of the fertiliser slurry. Therefore, the limitations of the present study can be eliminated by considering the energy equation in future studies.

## 5. ACKNOWLEDGEMENTS

This study did not benefit from any support.

## 6. CONFLICT OF INTEREST

Author approves that to the best of their knowledge, there is not any conflict of interest or common interest with an institution/organization or a person that may affect the review process of the paper.

## 7. AUTHOR CONTRIBUTION

Emre Aşkın ELİBOl has the full responsibility of the paper about determining the concept of the research, data collection, data analysis and interpretation of the results, preparation of the manuscript and critical analysis of the intellectual content with the final approval.

## 8. REFERENCES

Abu-Farah L., Al-Qaessi F., Schönbucher A., Cyclohexane/water dispersion behaviour in a stirred batch vessel experimentally and with CFD simulation. Procedia computer science 1(1), 655-664, 2010.

Achkari-Begdouri A., Goodrich P. R., Rheological properties of Moroccan dairy cattle manure. Bioresource technology 40(2), 149-156, 1992.

Bridgeman J., Computational fluid dynamics modelling of sewage sludge mixing in an anaerobic digester. Advances in Engineering Software 44(1), 54-62, 2012.

Cao X., Jiang K., Ding H., Yang P., Zhao Z., Xu G., Simulation and Analysis of Flow Field in Sludge Anaerobic Digestion Reactor based on Computational Fluid Dynamics. International Journal of Chemical Reactor Engineering 16(3), 2018.

Carreau P. J., De Kee D. C., Chhabra R. P., Rheology of polymeric systems: principles and applications, Carl Hanser Verlag GmbH Co KG, 2021.

Celik A. F., Elibol E. A., Turgut O., Senol H., Sillanpää M., Interpretation of possible biogas production capacity by investigating the effects of anaerobic digester tank geometry and angular velocity on flow characteristics. Environmental Science and Pollution Research: 1-15, 2024.

Fan W. B., Li W. G., Gong X. J., Zhang X. R., Evaluation of the effect of a hydraulic impeller in a flocculation basin on hydrodynamic behavior using computational fluid dynamics. Desalination and Water Treatment 54(4-5), 1361-1374, 2015.

Hoseini S., Najafi G., Ghobadian B., Akbarzadeh A., Impeller shape-optimization of stirred-tank reactor: CFD and fluid structure interaction analyses. Chemical Engineering Journal 413, 127497, 2021.

Kong J. Y., Wu Z. W., Hou Y., Wang X. D., Numerical simulation for solid-liquid two-phase flow in stirred vanadium leaching tank. Applied Mechanics and Materials 456, 314-319, 2014.

Launder B. E., Spalding D. B., Lectures in mathematical models of turbulence. 1972.

Mousavi S. E., Choudhury M. R., Rahaman M. S., 3-D CFD-PBM coupled modeling and experimental investigation of struvite precipitation in a batch stirred reactor. Chemical Engineering Journal 361, 690-702, 2019.

Oates A., Neuner T., Meister M., Borman D., Camargo-Valero M., Sleigh A., Fischer P., Modelling mechanically induced non-Newtonian flows to improve the energy efficiency of anaerobic digesters. Water 12(11), 2995, 2020.

Rasool A. A., Ahmad S. S., Hamad F., Effect of impeller type and rotational speed on flow behavior in fully baffled mixing tank. International Journal of Advanced Research (IJAR) 5(1), 1195-1208, 2017.

Sadino-Riquelme C., Hayes R. E., Jeison D., Donoso-Bravo A., Computational fluid dynamic (CFD) modelling in anaerobic digestion: General application and recent advances. Critical Reviews in Environmental Science and Technology 48(1), 39-76, 2018.

Servati P., Hajinezhad A., CFD simulation of anaerobic digestier to investigate sludge rheology and biogas production. Biomass Conversion and Biorefinery 10(4), 885-899, 2020.

Shen F., Tian L., Yuan H., Pang Y., Chen S., Zou D., Zhu B., Liu Y., Li X., Improving the mixing performances of rice straw anaerobic digestion for higher biogas production by computational fluid dynamics (CFD) simulation. Applied biochemistry and biotechnology 171(3), 626-642, 2013.

Sindall R., Bridgeman J., Carliell-Marquet C., Velocity gradient as a tool to characterise the link between mixing and biogas production in anaerobic waste digesters. Water science and technology 67(12), 2800-2806, 2013.

Thakur H., Verma N. K., Dhar A., Powar S., Investigation of continuous stirred tank reactors for improving the mixing in anaerobic digestion: A numerical study. Results in Engineering 19, 101317, 2023.

Versteeg H. K., Malalasekera W., An introduction to computational fluid dynamics: The finite volume method, England, Pearson, 2007.

Vilardi G., Verdone N., Production of metallic iron nanoparticles in a baffled stirred tank reactor: Optimization via computational fluid dynamics simulation. Particuology 52, 83-96, 2020.

Wang H., Aguirre-Villegas H. A., Larson R. A., Alkan-Ozkaynak A., Physical properties of dairy manure pre-and post-anaerobic digestion. Applied Sciences 9(13), 2703, 2019.

Wang J., Xue Q., Guo T., Mei Z., Long E., Wen Q., Huang W., Luo T., Huang R., A review on CFD simulating method for biogas fermentation material fluid. Renewable and Sustainable Energy Reviews 97, 64-73, 2018.

Wu B., CFD analysis of mechanical mixing in anaerobic digesters. Transactions of the ASABE 52(4), 1371-1382, 2009.

Wu B., CFD simulation of mixing in egg-shaped anaerobic digesters. Water research 44(5), 1507-1519, 2010.

Wu B., CFD investigation of turbulence models for mechanical agitation of non-Newtonian fluids in anaerobic digesters. Water research 45(5), 2082-2094, 2011.

Wu B., Large eddy simulation of mechanical mixing in anaerobic digesters. Biotechnology and Bioengineering 109(3), 804-812, 2012.

Wu B., Chen S., CFD simulation of non-Newtonian fluid flow in anaerobic digesters. Biotechnology and bioengineering 99(3), 700-711, 2008.